Dyes and Pigments 94 (2012) 403–409

Contents lists available at SciVerse ScienceDirect

Dyes and Pigments

journal homepage: www.elsevier.com/locate/dyepig

Synthesis, physical properties and self-assembly of conjugated donor–acceptor system based on tetrathiafulvalene and functionalized with binding sites

Chunyang Jia [a,*], Jiaqiang Zhang [a,b], Jingying Bai [b], Ligong Zhang [b], Zhongquan Wan [a], Xiaojun Yao [c]

[a] State Key Laboratory of Electronic Thin Films and Integrated Devices, School of Microelectronics and Solid-State Electronics, University of Electronic Science and Technology of China, Chengdu 610054, PR China
[b] Beijing Spacecrafts, China Academy of Space Technology, Beijing 100190, PR China
[c] State Key Laboratory of Applied Organic Chemistry, School of Chemistry and Chemical Engineering, Lanzhou University, Lanzhou 730000, PR China

ARTICLE INFO

Article history:
Received 6 December 2011
Received in revised form
12 February 2012
Accepted 14 February 2012
Available online 24 February 2012

Keywords:
Tetrathiafulvalene (TTF)
Donor–acceptor
Binding group
Intramolecular charge transfer
Self-assembly
Density functional theory (DFT)

ABSTRACT

A novel π-conjugated donor–acceptor compound (**1**) based on tetrathiafulvalene (TTF), which is functionalized with dipyridine, has been designed and synthesized. Spectroscopic and electrochemical behaviors of compound **1** demonstrate that the donor (TTF) unit strongly interacts with the electron-accepting group through the heteroaromatic bridge. The interaction of compound **1** with metallic ions can cause remarkable changes in the absorption and fluorescence spectra. DFT calculations reveal that the pyrazine ring is almost coplanar with the TTF plane, which is beneficial to the donor and acceptor electronic communication. Additionally, compound **1** can be self-assembled into nanostructures with smooth surface, hecto-nanometers in width and deca-micrometers in length.

1. Introduction

The chemistry of donor–acceptor (D–A) systems has been extensively explored over the past decades [1–8], much effort has been devoted to their synthesis in order to define structure–property relationships and generate functional molecular components for next-generation electronic and optical applications [9–13]. Electron transfer from D to A happens rapidly upon photoexcitation to generate a charge-separated species, subsequently charge recombination may proceed within the molecule to generate a charge transfer (CT) emission in certain cases [14,15], or it may be guided to proceed through an external circuit such as the design in dye-sensitized solar cells (DSSC) [16–19]. Undoubtedly, the electronic coupling between the donor and acceptor is a key parameter that determines the various important properties of D–A systems, which clearly depends on the nature of the donor, acceptor and linkage spacers.

Tetrathiafulvalene (TTF) and its derivatives feature unique π-donor properties and can be oxidized reversibly in two steps [20–22], hereby gaining heteroaromaticity. With this unique feature, TTF and its derivatives have been widely employed in numerous fields, for example, organic metals [23–25], molecular sensors [26–30], molecular logic gates [31,32], and so on.

Pyrazine moiety has been utilized as suitable π-conjugated bridge in charge transfer systems to optimize the electronic communication between TTF and acceptors. As demonstrated previously [30,33–37], upon introducing of a π-conjugated pyrazine as the linkage to construct TTF-π-A molecules, TTF and the acceptor moiety can interact with each other through the conjugated bridge, forming intramolecular charge transfer states.

To shed more light on the intramolecular charge transfer characteristics in nature, compound **1** based on TTF which bearing two pyridyl groups with pyrazine bridge has been taken into consideration. It is anticipated that (1) the conjugated structure may be beneficial to the electron communication between TTF and acceptor moieties; (2) the external metallic cation stimulus with pyridine and pyrazine groups could modulate the intramolecular charge transfer, resulting in remarkable changes in the absorption spectra and electrochemical properties. This paper is to study the synthesis and the physiochemical properties of compound **1**, expecting uniquely photo/electrochemical properties would be exhibited.

* Corresponding author. Tel.: +86 28 83202550; fax: +86 28 83202569.
E-mail address: cyjia@uestc.edu.cn (C. Jia).

0143-7208/$ – see front matter © 2012 Elsevier Ltd. All rights reserved.
doi:10.1016/j.dyepig.2012.02.008

2. Experimental section

2.1. General

Chemical reagents were obtained commercially and used without further purification except as noted elsewhere. All reactions were performed under N_2. Triethyl phosphite and toluene were dried and distilled over Na.

Mass spectra were measured on a Bruker Biflex III MALDI-TOF. ^{1}HNMR spectra were measured on a Bruker AV 300 at 300 MHz. Chemical shifts δ were calibrated against TMS as an internal standard. FT-IR spectra were recorded as KBr pellets on a Perkin-Elmer system 2000 spectrometer. Elemental analyses were performed on a Carlo-Erba-1106 instrument. Absorption spectra were measured with SHIMADZU (UV1700) UV–vis spectrophotometer. Fluorescence measurements were carried out with a SHIMADZU (RF-5301) fluorescence spectrophotometer in a 1 cm quartz cell. The cyclic voltammetric measurements were performed on CHI 660C system. The FE-SEM images of the self-assembly structure was measured by scanning electron microscope (SEM, FEI, inspect F)

2.2. Synthesis

The synthetic pathway is outlined in Scheme 1. In order to assure solubility, a TTF with dithiodecyl chains is employed. The target compounds (**1** and **2**) are obtained by direct condensation of 1,2-di(pyridin-2-yl)ethane-1,2-dione with the diamine precursors.

Tetrathiafulvalene-2,3-bis(2-pyridyl)pyrazine (**1**): A solution of compound **3** [33] (0.1 g, 0.16 mmol) and 1,2-di(pyridin-2-yl)ethane-1,2-dione (0.048 g, 0.23 mmol) in EtOH (20 mL) was refluxed for 3 h under N_2. After filtration, the precipitate was collected and purified by chromatography (CH_2Cl_2) to give compound **1** as a mauve solid (80%), mp 109 °C. ^{1}HNMR ($CDCl_3$, 300 MHz) δ: 0.86 (t, J = 6.6, 6H, 2×CH_3), 1.25 (m, 24H, 12×CH_2), 1.39 (m, 4H, 2×CH_2), 1.62 (m, 4H, 2×CH_2), 2.84 (t, J = 7.3, 4H, 2×SCH_2), 7.22 (m, 2H, aromatic), 7.80 (m, 2H, aromatic), 7.89(d, J = 7.8, 2H, aromatic), 7.99 (s, 2H, aromatic), 8.37 (d, J = 4.3, 2H, aromatic). Selected IR data (cm^{-1}, KBr pellet): 2920, 2850, 1638, 1583 1468, 1432, 1350, 1198, 1098, 1075, 1002, 887, 859, 831, 789, 775, 742, 725, 553; MS (MALDI-TOF) calcd. For $C_{42}H_{52}N_4S_6$: 804.25, found 805.2 $[M]^+$; elemental analysis calcd. (%) for $C_{42}H_{52}N_2S_6$: C, 62.64; H, 6.51; N, 6.96; found: C, 62.44; H, 6.59; N, 6.76.

2.3. Self-assembly

The self-assembled micro-nanostructures are prepared by the similar process as references [38,39]. Compound **1** was dissolved in $CHCl_3$ as a concentration of 1.2×10^{-3} M. Next 20 drops of the solution were injected into 25 mL of methanol with vigorous stirring at 358 K. After being stirred for 30 min, the samples were cooled to room temperature and undisturbed overnight to stabilize the crystal growth. The morphology of the self-assembled micro/nanostructures was observed by field emission SEM (SEM, FEI, inspect F). For FE-SEM studies, a few drops of the solution were placed onto silicon substrate, and the solvent was left to evaporate. To minimize sample charging, an ultrathin layer of Au was deposited onto the samples before FE-SEM examination.

3. Results and discussion

3.1. Synthesis

Compound **1** can be synthesized in 80% yield via the direct condensation of 1,2-di(pyridin-2-yl)ethane-1,2-dione with 5,6-diamino-2-[4,5-bis(decylthio)-1,3-dithio-2-ylidene]-benzo[d]-1,3-dithiole (**3**) in ethanol, as shown in Scheme 1. Compound **2** [40] was synthesized as the reference. ^{1}HNMR spectra, MS spectra and elemental analysis confirmed the structure of the D-π-A conjugated system.

3.2. Cyclic voltammetry (CV)

It has been well known that TTF derivatives can undergo two successively reversible one-electron oxidations to the $TTF^{+\bullet}$ radical and TTF^{2+} species, thus their redox properties have received extensive attention for application as ion sensors [41,42]. The CV measurements of this work were carried out in the mixed solvent of CH_2Cl_2/MeCN (3:2 in volumes). Fig. 1 presents the reversible CV curve of compound **1**. Two redox waves were detected, $E_{1/2(1)} = 0.71$ V and $E_{1/2(2)} = 1.09$ V, corresponding to the TTF/$TTF^{\bullet+}$ and $TTF^{\bullet+}$/TTF^{2+} redox couples. They are both anodically shifted as compared to the first and second oxidation waves of compound **3**, indicating compound **1** is more difficult to be oxidized than compound **3**. The results reveal strong intramolecular electron communication between donor and acceptor units in the ground state. The partially intramolecular charge transfer from the TTF unit

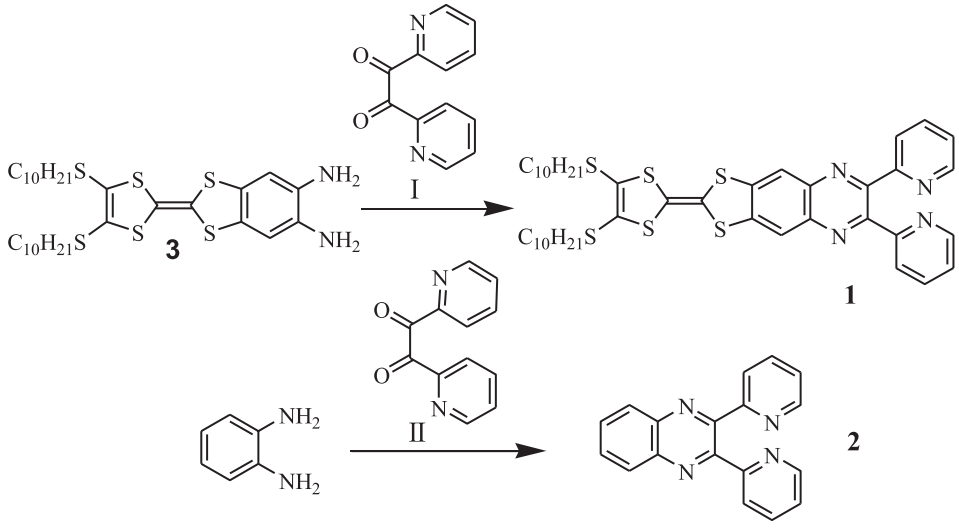

Scheme 1. Synthetic routes of compounds **1** and **2**.

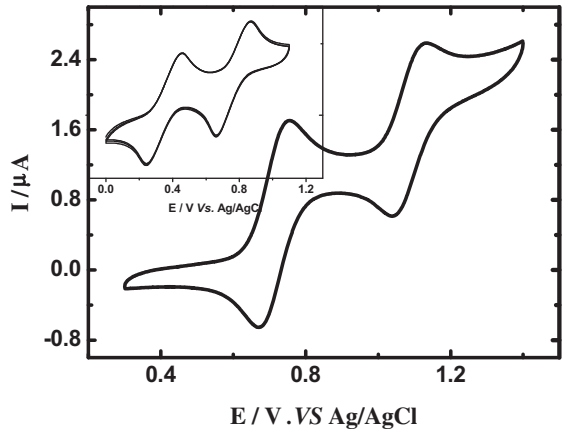

Fig. 1. Cyclic voltammogram of compounds **1** and **3** (inset) in CH_2Cl_2/MeCN (3:2 in volumes) (3.8×10^{-4} M, scanning rate 30 mV/s) with platinum wires as working and counter electrodes, respectively, Ag/AgCl as a reference electrode, and *n*-Bu_4NPF_6 (0.1 M) as a supporting electrolyte.

to the acceptor moiety decreases the electron density of the TTF ring and makes the oxidation of TTF less favorable.

To further investigate the property of compound **1**, cation titration was carried out. When metallic cations of Co^{2+}, Mn^{2+}, Mg^{2+} and Ni^{2+} were added, $E_{1/2(1)}$ and $E_{1/2(2)}$ of compound **1** did not shift obviously (Fig. S1 and Table S1, ESI). The electrochemical behaviors indicate that the interactions between these cations with compound **1** are very weak under the experimental conditions. However, it is interestingly found that with the addition of Zn^{2+}, Hg^{2+}, Cd^{2+} cations into the solution of **1** lead to an obvious potential shift of $E_{1/2(1)}$ of the TTF moiety (Fig. S1 and Table S1, ESI). Similar potential shifts are found for Ag^{+} and Cu^{2+}, but the curve is not clarified (Fig. S1 and Table S1, ESI).

3.3. Absorption Spectra

The UV–vis absorption data of **1**, **2** and **3** are collected in Fig. 2(a). By comparing with the spectra of **2** and **3**, compound **1** shows a wide absorption in the whole range from 400 to 600 nm, with the maximum at $\lambda = 480$ nm, which results from an intramolecular charge transfer (ICT) interaction between the donor and the acceptor, according to the previous literature [33,43,44]. In compound **1**, the dipyridine and pyrazine units display an electron withdrawing effect and the TTF exhibits a strong electron-donating effect. Since these units are linked directly by a conjugated bridge, the two electro-active moieties can readily interact with each other, which is beneficial to the ICT interaction.

Chemical oxidation of compound **1** in CH_2Cl_2 is carried out by successive addition of $Fe(ClO_4)_3 \bullet 6H_2O$ as oxidizing reagent. UV–vis spectra of the reaction system are recorded. Upon addition of Fe^{3+}, the absorption band centered at 480 nm is shifted to a lower energy area, and a new band at 700–1000 nm is formed [Fig. 2(b)]. Upon further oxidation, a new peak at $\lambda_{max} = 474$ nm has emerged. According to previous studies [45,46], the absorption bands around 700 nm to 1000 nm could be ascribed to the radical cation of TTF ($TTF^{\bullet+}$) in compound **1**, the band of $\lambda_{max} = 474$ nm could be ascribed to the dication of TTF^{2+}. The decreasing of the absorption at 480 nm is accompanied by the growth of a new band which is maximum at 560 nm. The red-shifted of this band just corresponds to the decrease of the HOMO-LUMO gap, which may be attributed to the interaction of Fe^{3+} or the reduced Fe^{2+} cations with the dipyridine SP^2 nitrogens to form a stronger electron acceptor. This phenomenon is further confirmed by the following experimental results.

It is expected that compound **1** could coordinate with different metal ions through the pyridine and pyrazine groups (according to the reported results [47,48], the binding sites of the compound could be contributed to the sp^2-hybridized nitrogens on the

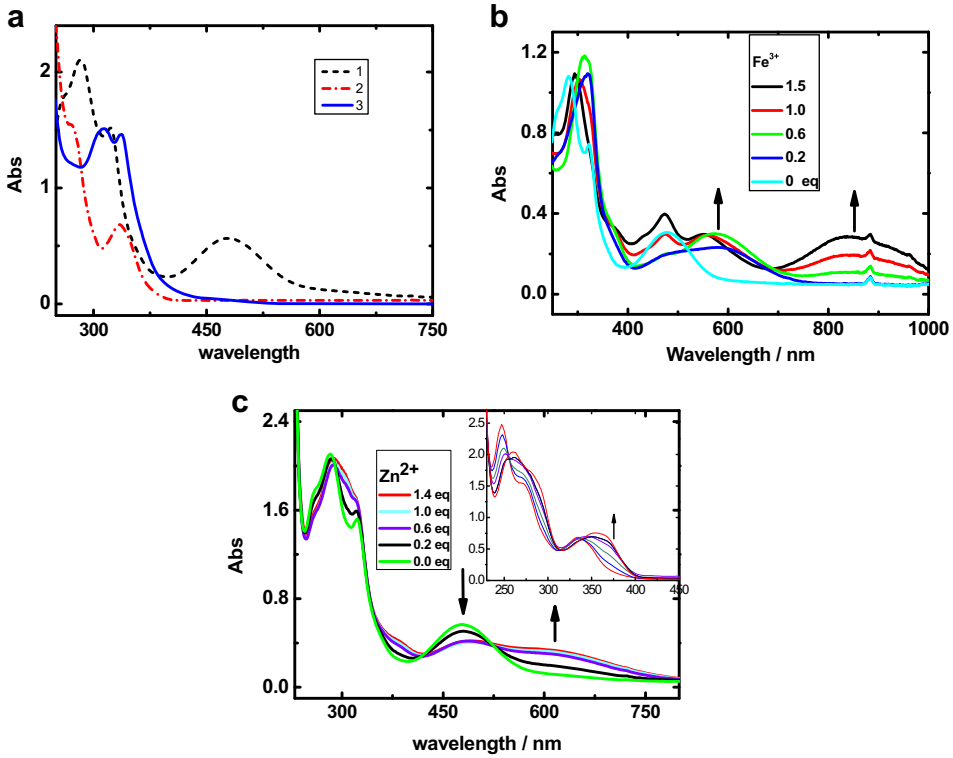

Fig. 2. UV–vis spectra of compound **1** (2.4×10^{-5} M) in different conditions: (a) the spectra of compounds **1**, **2** (7.5×10^{-5} M) and **3** (5.7×10^{-5} M) in CH_2Cl_2; (b) Absorption spectra of compound **1** in CH_2Cl_2 with increasing of Fe^{3+} [$Fe(ClO_4)_3 \bullet 6H_2O$, 3.0×10^{-3} M in CH_3OH]; (c) Absorption spectra of compounds **1** and **2** (inset, 7.5×10^{-5} M) in CH_2Cl_2 with increasing of Zn^{2+} [$Zn(NO_3)_2 \bullet 6H_2O$, 4.5×10^{-3} M in CH_3OH].

pyrazine and pyridine groups), which should favor the electronic communication between TTF and the acceptor units. With this goal in mind, titrations of compound **1** in CH_2Cl_2 solution with Zn^{2+}, Cu^{2+}, Ag^{+}, Ni^{2+}, Mg^{2+}, Hg^{2+} and Mn^{2+} ions were undertaken, and the changes in their absorption spectra were recorded.

The salient results obtained from compound **1** are the remarkable sensing and coordinating properties in the case of Zn^{2+}, Cu^{2+}, Ag^{+}, Ni^{2+}. Upon addition of Zn^{2+} to the solution of **1**, the decreasing of the absorption at 480 nm is accompanied by a new absorption band at 550–750 nm centered at 605 nm (Fig. 2(c)). The intramolecular charge transfer responsive to the external cation stimulus exhibits a bathochromic shift. Obviously, the complexation of compound **1** with Zn(II) cations reduces the electron density on the pyridine and pyrazine ring successively, which further enhances the electron-acceptor character of the compound. Prompting **1** to be a stronger polarized D-π-A system and the results inducing the absorption of ICT shifted to a lower energy direction. The red-shifted in the absorption spectra suggests the strongly electronic coupling between donor and acceptor units in compound **1**. Similar results were obtained in the titrations of **1** with Cu^{2+}, Ag^{+} and Ni^{2+} salts (Table 1, Fig. S2 ESI). Other tested metal cations, including Mg^{2+}, Hg^{2+}, Mn^{2+} do not induce any distinct change in their UV–vis spectra (Fig. S3, ESI).

3.4. Fluorescence spectra

To get further insight into the binding properties of compounds **1** and **2** with metallic cations, fluorescence spectra of compounds **1** and **2** have been investigated (Fig. 3). It shows that the fluorescence of compound **2** is increased with the amount of the Zn^{2+}. However, after addition of Zn^{2+}, the weak fluorescence of compound **1** starts to decrease. The results could be owed to the complexation of Zn^{2+} with pyridine and pyrazine groups in compound **1**. These results also match with the UV–vis behavior of compound **1**.

3.5. Theoretical calculations

To gain insight into the molecular structure and electronic configurations, compound **1** is further examined by theoretical calculations. The peripherally longer alkyl groups are removed for simplification (labeled as model **1**) as they are not expected to have significantly affects on the conformations and energy levels. The molecular geometries are optimized by using B3LYP/6-31G** basis set initially, then the excited states are calculated at this geometry in gas phase using TD-DFT with the B3LYP/6-31G** basis set. All calculations have been performed with the Gaussian 09 package [49].

After discovering that the lowest energy conformations of model **1** may involve the orientation of the pyridine moieties in or out of the molecular center, we calculated the different possible orientations of the pyridines and allowed the system to relax without constraints. Eight new local minima were identified and the conformations are illustrated in Fig. 4, and the geometric properties and relative energy of the minima are reported in Table 2.

Table 1
The cation-induced absorption peak of compound **1**.

Metallic cations	$\lambda_{max\text{-}ICT}$
Zn^{2+}	605
Cu^{2+}	575
Ag^{2+}	586
Ni^{2+}	603

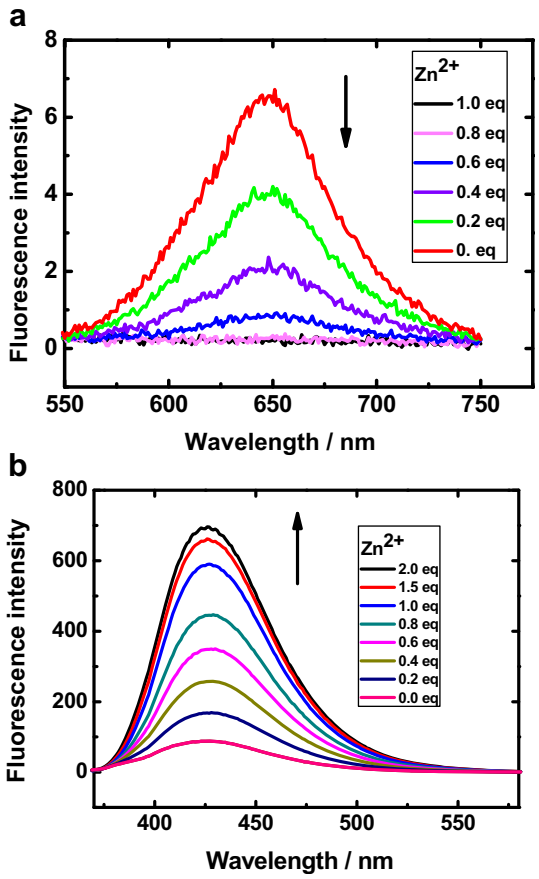

Fig. 3. Fluorescence spectra of compounds **1** and **2** in CH_2Cl_2 (2.4×10^{-5} M, 7.5×10^{-5} M, respectively) with increasing of $Zn(NO_3)_2 \bullet 6H_2O$ (3.0×10^{-3} M in MeOH); (a) Fluorescence spectra of compound **1**, the excitation wavelength is 491 nm, (b) Fluorescence spectra of compound **2**, the excitation wavelength is 358 nm.

According to the optimized molecular geometries, the conformations of heteroaromatic pyrazine bridge and TTF ring are nearly coplanar, but the two pyridine rings are twisted due to the steric hindrance. All of the conformations are higher in energy than conformation **A**/**B**, the conformations where two pyridines are oriented away from the center (out–out conformation). Conformation **C**/**D**, in which both of the pyridines are oriented in the center of the molecule, have much higher in energy than that of conformation **A**/**B** (23.8 kJ/mol). Conformations **E**/**F** and **G**/**H** with one of the pyridine moieties in and another is out of the molecular center. This leads to the higher energy conformations (9.75 and 10.0 kJ/mol above **A**/**B**, respectively).

A particularly interesting feature in the frontier molecular orbits of the conformations is the localization and spatial separation of the HOMO and the LUMO (Fig. S4, ESI). The electron density of HOMO is mainly located on the TTF moiety and extended along the bridge to the central region of the molecule, while the LUMO is mainly located on dipyridine and pyrazine units. It can be seen that there is an overlap between the HOMO and LUMO on the quinoxaline group, which is a prerequisite to increase the probability of the charge transfer transitions and lead to a positive shift of the redox potentials of the donor subunit.

The broad absorption (Fig. 2) at lower energy has a large intramolecular charge transfer character, which can be demonstrated by analyzing the electron density. Upon photo excitation, an electron migrates from donor to acceptor to form a charge-

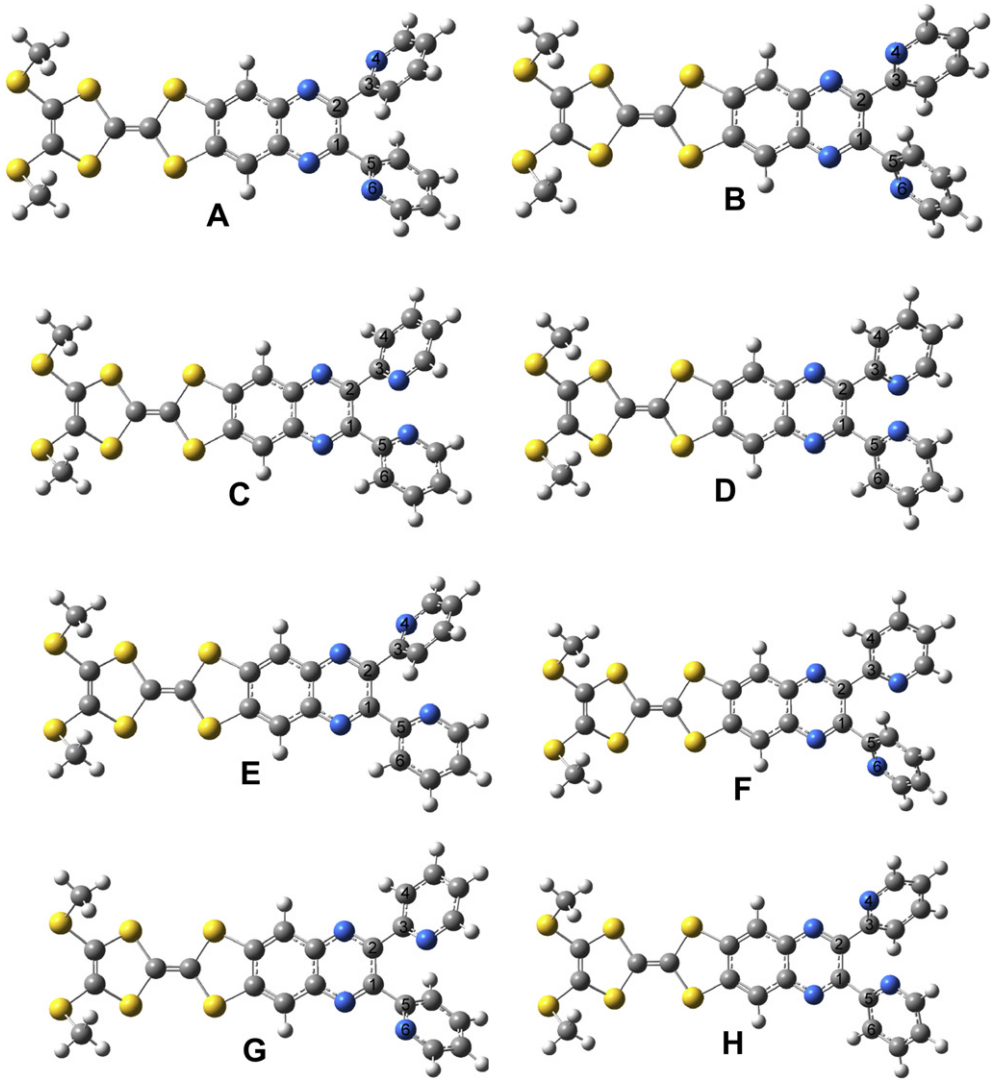

Fig. 4. Computed minima conformations of **A**–**H** for model **1**.

separated dipolar state. The electron density of donor and acceptor is heavily coupled with the orbitals in the central pyrazine linkage, which suggests that this material is one of good candidates to be investigated in optoelectronic devices.

TD-DFT studies were performed in order to interpret the optical properties of compound **1**. The most relevant calculated electronic transitions of the conformations are presented in Table S2 (ESI). The excited state data can be used to interpret the UV–vis spectra of compound **1**.

Table 2
Energies and geometrical properties of the eight minima conformations reported in Fig. 4, calculated at B3LYP/6-31G** levels.

Conformation	Diangle α (1-2-3-4)	Diangle β (2-1-5-6)	Energy [AU]
A	129.75034	129.50404	−3532.31389551
B	129.50544	−129.74488	−3532.31389552
C	146.48943	146.63488	−3532.32295061
D	−146.63496	−146.48951	−3532.32295061
E	130.35072	153.26638	−3532.31760748
F	−153.25181	−130.36172	−3532.31760749
G	152.97867	130.24951	−3532.31770628
H	−130.24334	−152.97562	−3532.31770623

The experimental broad band at 480 nm of compound **1** is expected to have contributions from the transitions with the higher oscillator strength value and is assigned to a transition from HOMO to LUMO (93%). The second observed band (experimental value

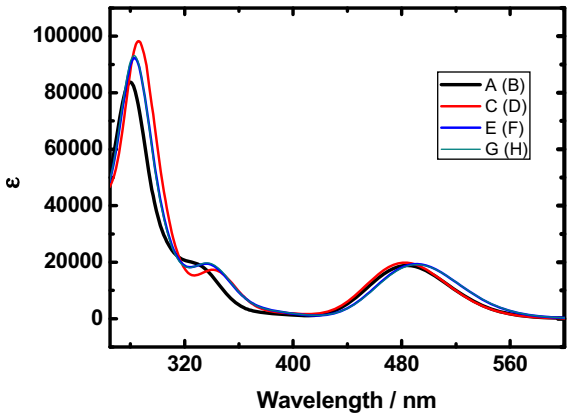

Fig. 5. Electronic absorption spectra of conformations **A**–**H**.

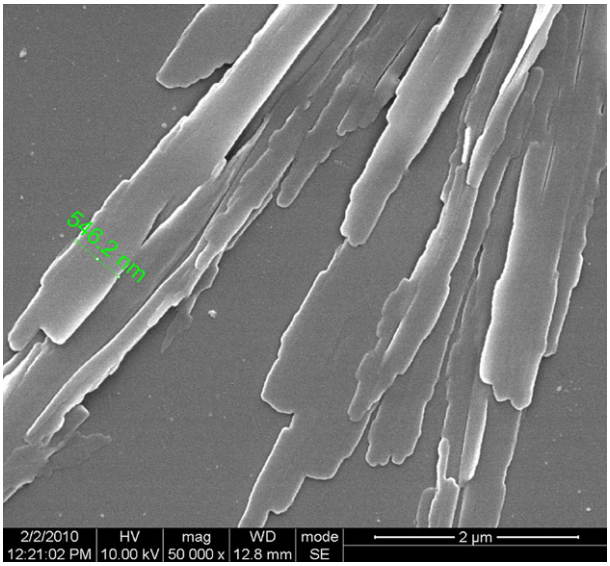

Fig. 6. FE-SEM image of self-assembled 2D nanostrips of compound **1**.

283 nm) is a mixed transition (the involved orbitals in these transitions are represented in Table S2, ESI). This is in good agreement with the higher and lower energy band in the UV–vis spectra of compound **1**. Therefore, there is reasonable agreement between theoretical and experimental results (Fig. 5), indicating that the absorption band from 400 to 600 nm belongs to the intramolecular charge transfer absorption

3.6. Self-assembly investigation

To gain a direct insight into the self-assembly characteristic of compound **1**, scanning electron microscopy (SEM) is used to study the results. The compound forms straight and short 2D nanostrips with hecto-nanometers in width, deca-micrometers in length and the surface is smooth (Fig. 6). Unfortunately, the metallic-complexes of **1** are unstable compounds which are immediately hydrolyzed and decomposed in the air. Thus, the self-assembly structures of compound **1** with different metal ions could not obtained by the self-assemblization method. However, it is expected that the functional organic micro-nanostructures of compound **1** are to be used as building blocks for next generation of organic semiconductor nanodevices, and the in-depth investigations of the self-assembly nanostrips are in progress.

4. Conclusion

In conclusion, a new TTF-based donor–acceptor compound **1** which is functionalized with pyrazine and linked by pyrazine bridge has been prepared. Spectroscopic, electrochemical, metallic cations binding and theoretical studies have demonstrated that the pyrazine ring is greatly facilitated to the electronic communication between TTF moiety and acceptor unit, thus leading to intramolecular charge transfer. The interaction of pyridyl-substituted TTF compound with metallic ions can significantly cause the remarkable changes in the absorption and fluorescence spectra. The calculated structure of compound **1** reveals that the pyrazine ring is almost coplanar to the plane of TTF, which is beneficial to the donor and acceptor electronic communication. The self-assembly nanostructures of compound **1** have potential applications in future optoelectronic devices.

Acknowledgements

We thank the National Natural Science Foundation of China (Grant Nos. 20602005, 20873015), the Innovation Funds of State key Laboratory of Electronic Thin Films and Integrated Device (Grant No. CXJJ201104), the Fundamental Research Funds for the Central Universities (Grant No. ZYGX2010J035) and Beijing National Laboratory for Molecular Sciences (BNLMS) for financial support.

Appendix. Supplementary material

Supplementary material associated with this article can be found, in the online version, at doi:10.1016/j.dyepig.2012.02.008.

References

[1] Sun F, Hu F, Zhang GX, Zhang DQ. Metal-ion-promoted electron transfer between tetrathiafulvalene and quinone units within a calix[4]arene framework and tuning through coordination of the neighboring crown ether with a sodium cation. Chem Asian J 2012;7:183–9.
[2] Jia HP, Ding J, Ran YF, Liu SX, Blum C, Petkova I, et al. Targeting p-conjugated multiple donor-acceptor motifs exemplified by tetrathiafulvalene-linked quinoxalines and tetrabenz[bc, ef, hi, uv]ovalenes: synthesis, spectroscopic, electrochemical, and theoretical characterization. Chem Asian J 2011;6:3312–21.
[3] Tan LX, Zhang GX, Zhang DQ, Zhu DB, Tan LXZG, Zhang DQ, Zhu DB. Linear and cyclic tetrathiafulvalene–naphthalenediimide donor–acceptor molecules: metal ions-promoted electron transfer. J Org Chem 2011;76:9046–52.
[4] Santos J, Illescas BM, Martin N, Adrio J, Carretero JC, Viruela R, et al. A fully conjugated TTF-π-tcaq system: synthesis, structure, and electronic properties. Chem Eur J 2011;17:2957–64.
[5] Sun F, Hu F, Zhang GX, Zheng QY, Zhang DQ. Calix[4]arenes with electroactive tetrathiafulvalene and quinone units: metal-ion-promoted electron transfer. J Org Chem 2011;76:6883–8.
[6] Takano Y, Herranz MA, Martin N, Rojas GM, Guldi DM, Kareev IE, et al. Electron donor-acceptor interactions in regioselectively synthesized exTTF$_2$-C$_{70}$(CF$_3$)$_{10}$ dyads. Chem Eur J 2010;16:5343–53.
[7] Park JS, Karnas E, Ohkubo K, Chen P, Kadish KM, Fukuzumi S, et al. Ion-mediated electron transfer in a supramolecular donor-acceptor ensemble. Science 2010;329:1324–7.
[8] Takano Y, Herranz MA, Martin N, Radhakrishnan SG, Guldi DM, Tsuchiya T, et al. Donor-acceptor conjugates of lanthanum endohedral metallofullerene and π-extended tetrathiafulvalene. J Am Chem Soc 2010;132:8048–55.
[9] Martin N, Sánchez L, Herranz MÁ, Illescas B, Guldi DM. Electronic communication in tetrathiafulvalene (TTF)/C$_{60}$ systems: toward molecular solar energy conversion materials. Acc Chem Res 2007;40:1015–24.
[10] Sommer M, Huettner S, Thelakkat M. Donor-acceptor block copolymers for photovoltaic applications. J Mater Chem 2010;20:10788–97.
[11] Li Y, Xue L, Li H, Li Z, Xu B, Wen S, et al. Energy level and molecular structure engineering of conjugated donor–acceptor copolymers for photovoltaic applications. Macromolecules 2009;42:4491–9.
[12] Traber B, Wolff JJ, Rominger F, Oeser T, Gleiter R, Goebel M, et al. Hexasubstituted donor-acceptor benzenes as nonlinear optically active molecules with multiple charge-transfer transitions. Chem Eur J 2004;10:1227–38.
[13] Oliva MM, Casado J, Raposo MMM, Fonseca AMC, Hartmann H, Hernández V, et al. Structure-property relationships in push–pull amino/cyanovinyl end-capped oligothiophenes: quantum chemical and experimental studies. J Org Chem 2006;71:7509–20.
[14] Chen S, Xu X, Liu Y, Qiu W, Yu G, Wang H, et al. New organic light-emitting materials: synthesis, thermal, photophysical, electrochemical, and electroluminescent properties. J Phy Chem C 2006;111:1029–34.
[15] Goes M, Verhoeven JW, Hofstraat H, Brunner K. OLED and PLED devices employing electrogenerated, intramolecular charge-transfer fluorescence. Chem Phys Chem 2003;4:349–58.
[16] Liu B, Zhu W, Zhang Q, Wu W, Xu M, Ning Z, et al. Conveniently synthesized isophorone dyes for high efficiency dye-sensitized solar cells: tuning photovoltaic performance by structural modification of donor group in donor-π-acceptor system. Chem Commun; 2009:1766–8.
[17] Wenger S, Bouit P-A, Chen Q, Teuscher J, Di Censo D, Humphry-Baker R, et al. Efficient electron transfer and sensitizer regeneration in stable π-extended tetrathiafulvalene-sensitized solar cells. J Am Chem Soc 2010;132:5164–9.
[18] Campbell WM, Burrell AK, Officer DL, Jolley KW. Porphyrins as light harvesters in the dye-sensitised TiO$_2$ solar cell. Coord Chem Rev 2004;248:1363–79.
[19] Tian ZF, Huang MH, Zhao B, Huang H, Feng XM, Nie YJ, et al. Low-cost dyes based on methylthiophene for high-performance dye-sensitized solar cells. Dyes Pigments 2010;87:181–7.
[20] Jeppesen JO, Nielsen MB, Becher J. Tetrathiafulvalene cyclophanes and cage molecules. Chem Rev 2004;104:5115–32.
[21] Canevet D, Salle M, Zhang G, Zhang D, Zhu D. Tetrathiafulvalene (TTF) derivatives: key building-blocks for switchable processes. Chem Commun; 2009:2245–69.

[22] Iyoda M, Hasegawa M, Miyake Y. Bi-TTF, bis-TTF, and related TTF oligomers. Chem Rev 2004;104:5085–114.
[23] Bouguessa S, Gouasmia AK, Golhen S, Ouahab L, Fabre JM. Synthesis and characterization of TTF-type precursors for the construction of conducting and magnetic molecular materials. Tetrahedron Lett 2003;44:9275–8.
[24] Dressel M, Drichko N. Optical properties of two-dimensional organic conductors: signatures of charge ordering and correlation effects. Chem Rev 2004;104:5689–716.
[25] Jérome D. Organic conductors: from charge density wave TTF–TCNQ to superconducting $(TMTSF)_2PF_6$. Chem Rev 2004;104:5565–92.
[26] Lyskawa J, Le Derf F, Levillain E, Mazari M, Salle M. Tetrathiafulvalene-based podands for Pb^{2+} recognition. Eur J Org Chem; 2006:2322–8.
[27] Hansen TK, Stein PC. Én route to molecular sensors based on TTF. Synth Met 1993;56:1972–7.
[28] Liu L-H, Zhang H, Li A-F, Xie J-W, Jiang Y-B. Intramolecular charge transfer dual fluorescent sensors from 4-(dialkylamino)benzanilides with metal binding site within electron acceptor. Tetrahedron 2006;62:10441–9.
[29] Balandier JY, Belyasmine A, Salle M. Tetrathiafulvalene-imine-pyridine assemblies for Pb^{2+} recognition. Eur J Org Chem; 2008:269–76.
[30] Goze C, Dupont N, Beitler E, Leiggener C, Jia H, Monbaron P, et al. Ruthenium(II) coordination chemistry of a fused donor–acceptor ligand: synthesis, characterization, and photoinduced electron-transfer reactions of $[\{Ru(bpy)_2\}n(TTF\text{-}ppb)](PF_6)_{2n}$ ($n = 1, 2$). Inorg Chem 2008;47:11010–7.
[31] Sun W, Xu C-H, Zhu Z, Fang C-J, Yan C-H. Chemical-driven reconfigurable arithmetic functionalities within a fluorescent tetrathiafulvalene derivative. J Phy Chem C 2008;112:16973–83.
[32] Fang C-J, Zhu Z, Sun W, Xu C-H, Yan C-H. New TTF derivatives: several molecular logic gates based on their switchable fluorescent emissions. New J Chem 2007;31:580–6.
[33] Jia C, Liu S-X, Tanner C, Leiggener C, Neels A, Sanguinet L, et al. An experimental and computational study on intramolecular charge transfer: a tetrathiafulvalene-fused dipyridophenazine molecule. Chem Eur J 2007;13:3804–12.
[34] Guégano X, Kanibolotsky AL, Blum C, Mertens SFL, Liu S-X, Neels A, et al. Pronounced electrochemical amphotericity of a fused donor-acceptor compound: a planar merge of TTF with a TCNQ-type bithienoquinoxaline. Chem Eur J 2009;15:63–6.
[35] Jia C, Zhang J, Zhang L, Yao X. A novel conjugated donor-acceptor system based on tetrathiafulvalene merging pyrene unit: synthesis, physical properties and theoretical calculations. Heterocycles 2011;83:1527–34.
[36] Jia C, Zhang J, Zhang L, Yao X. Structure-property relationships in conjugated donor-acceptor systems functionalized with tetrathiafulvalene. New J Chem 2011;35:1876–82.
[37] Wan Z, Jia C, Zhang J, Yao X, Shi Y. Highly conjugated donor–acceptor dyad based on tetrathiafulvalene covalently attached to porphyrin unit. Dyes Pigments 2012;93:1456–62.
[38] Zhang X, Zhang X, Wang B, Zhang C, Chang JC, Lee CS, et al. One- or semi-two-dimensional organic nanocrystals induced by directional supramolecular interactions. J Phy Chem C 2008;112:16264–8.
[39] Chen Y, Zhu B, Zhang F, Han Y, Bo Z. Hierarchical supramolecular self-assembly of nanotubes and layered sheets. Angew Chem Int Ed 2008;47:6015–8.
[40] Goodwin HA, Lions F. Tridentate chelate compounds. II[1]. J Am Chem Soc 1959;81:6415–22.
[41] Lu H, Xu W, Zhang D, Zhu D. Highly effective phosphate electrochemical sensor based on tetrathiafulvalene. Chem Commun; 2005:4777–9.
[42] Bejger C, Park JS, Silver ES, Sessler JL. Tetrathiafulvalene diindolylquinoxaline: a dual signaling anion receptor with phosphate selectivity. Chem Commun 2010;46:7745–7.
[43] Jaggi M, Blum C, Marti BS, Liu S-X, Leutwyler S, Decurtins S. Annulation of tetrathiafulvalene to the bay region of perylenediimide. Org Lett 2010;12:1344–7.
[44] Jaggi M, Blum C, Dupont N, Grilj J, Liu S-X, Hauser Jr A, et al. A compactly fused π-conjugated tetrathiafulvalene-perylenediimide donor-acceptor dyad. Org Lett 2009;11:3096–9.
[45] Zhao YP, Wu LZ, Si G, Liu Y, Xue H, Zhang LP, et al. Synthesis, spectroscopic, electrochemical and Pb^{2+}-binding studies of tetrathiafulvalene acetylene derivatives. J Org Chem 2007;72:3632–9.
[46] Andersson AS, Diederich F, Nielsen MB. Acetylenic tetrathiafulvalene-dicyanovinyl donor-acceptor chromophores. Org & Biomol Chem 2009;7:3474–80.
[47] Zhou Q-X, Lei W-H, Sun Y, Chen J-R, Li C, Hou Y-J, et al. $[Ru(bpy)_{3-n}(dpb)_n]^{2+}$: unusual photophysical property and efficient DNA photocleavage activity. Inorg Chem 2010;49:4729–31.
[48] Higgins SLH, White TA, Winkel BSJ, Brewer KJ. Redox, spectroscopic, and photophysical properties of Ru–Pt mixed-metal complexes incorporating 4,7-diphenyl-1,10-phenanthroline as efficient DNA binding and photocleaving agents. Inorg Chem 2010;50:463–70.
[49] Frisch MJ, Trucks GW, Schlegel HB, Scuseria GE, Robb MA, Cheeseman JR, et al, Gaussian 09 RA. Wallingford CT: Gaussian, Inc.; 2009.